Coarsening mechanisms in surface morphological evolution

2002 J. Phys.: Condens. Matter 14 4177

(http://iopscience.iop.org/0953-8984/14/16/309)

INSTITUTE OF PHYSICS PUBLISHING JOURNAL OF PHYSICS: CONDENSED MATTER

J. Phys.: Condens. Matter **14** (2002) 4177–4185 PII: S0953-8984(02)29088-8

Coarsening mechanisms in surface morphological evolution

Thomas Michely[1,5], **Matthias Kalff**[2,6], **George Comsa**[3], **Matthias Strobel**[1,4,7] **and Karl-Heinz Heinig**[4]

[1] I. Physikalisches Institut, RWTH-Aachen, 52056 Aachen, Germany
[2] Institut für Grenzflächenforschung und Vakuumphysik, Forschungszentrum Jülich, 52425 Jülich, Germany
[3] Institut für Theoretische und Physikalische Chemie, Universität Bonn, 53115 Bonn, Germany
[4] Institut für Ionenstrahlphysik und Materialforschung, Forschungszentrum Rossendorf, 01314 Dresden, Germany

E-mail: michely@physik.rwth-aachen.de

Received 25 September 2001, in final form 12 December 2001
Published 11 April 2002
Online at stacks.iop.org/JPhysCM/14/4177

Abstract

On the basis of a temperature-dependent, quantitative scanning tunnelling microscopy analysis of homoepitaxial growth and erosion of Pt(111), the atomic scale mechanisms responsible for coarsening of mounds and pits are identified. For an extended coarsening regime on Pt(111), step-edge diffusion including the thermal creation of species that are mobile along steps is found to be decisive. Only when step adatoms are thermally excited at kink sites does coarsening take place. It is argued that for many low-index surfaces this coarsening mechanism is likely to be operative. Instead of the surface diffusion current driven by changes in surface curvature frequently assumed in phenomenological theory as the origin of coarsening, it appears thus that even at high temperatures coarsening is driven only by differences in curvature along contours of constant height. At lower temperatures, when no mobile species are thermally created at steps on Pt(111), only an initial coarsening takes place, as long as the step-edge barrier to the descent of adatoms is small.

Destabilization of an initially smooth surface by homoepitaxial growth or ion erosion has become a topic of intense experimental and theoretical research interest (e.g. [1–20]). For low-index crystal surfaces and normal particle incidence, destabilization results in a morphology of mounds and/or pits. As key mechanisms of surface destabilization, asymmetries of incorporation into ascending and descending steps for both adatoms and vacancies have been identified [1, 2]. The surface destabilization is frequently [6, 8, 11], though not always [13], accompanied by

[5] Author to whom any correspondence should be addressed.
[6] Present address: Continental Teves AG, Guerickestrasse 7, 60488 Frankfurt, Germany
[7] Present address: PSI AG, Boschweg 6, 63741 Aschaffenburg, Germany

coarsening of the surface structure, i.e. an increase in the separation of the characteristic surface features. Phenomenological theory [4,12,17] assumes coarsening to rely on a surface diffusion current $\vec{j}_{eq} \sim \vec{\nabla}(\nabla^2 h)$ (h is the surface height) driven by curvature-dependent differences of the surface chemical potential. Depending on the surface crystallography, scaling exponents $1/z$ between $1/4$ and $1/3$ are expected for the coarsening of the characteristic surface length scale λ with removed or deposited amount Θ: $\lambda \sim \Theta^{1/z}$ [4, 12, 17]. For a crystalline surface, diffusion may be due to detachment of atoms from steps, due to their migration over terraces and subsequent reattachment or due to the motion of atoms along step edges without the need to lose contact with the step. It is *a priori* not clear whether both or only one—and then which one—of these processes may be linked to the above-mentioned phenomenological picture. Recent theoretical work stresses the importance of step-edge diffusion for coarsening [14–16], while recent experimental work favours step atom detachment [8, 11]. Even in the absence of surface diffusion, coarsening was suggested to take place due to fluctuations in the impinging particle flux [14] or due to funnelling [5, 7]. Here two examples of surface morphological evolution are discussed, homoepitaxial growth on Pt(111) between 400 and 480 K [13] and ion erosion of Pt(111) in the temperature range between 600 and 800 K [18, 19]. It will be seen that coarsening in the presence of surface diffusion is dominated by step-edge diffusion, if step-edge diffusion allows for step fluctuations even in the absence of particle impingement. Without such fluctuations no coarsening is found for large asymmetries of particle incorporation into steps.

The experiments were performed in a variable-temperature STM apparatus with a background pressure below 5×10^{-11} mbar. A clean Pt(111) sample with a relative density of step atoms below 1×10^{-3} was prepared prior to each experiment by ion bombardment at 970 K, followed by brief annealing to 1170 K. For homoepitaxial growth, evaporation was performed from a carefully cleaned Pt wire [13]. The pressure during Pt evaporation and subsequent STM imaging remained always $\leqslant 3 \times 10^{-11}$ mbar. The deposition was performed at a rate $R = (7 \pm 3) \times 10^{-3}$ ML s^{-1} (ML standing for monolayer) in the temperature range of $T = 400$–480 K, the conditions known from previous experiments to lead to three-dimensional growth. The experiments were performed at $T = 440$ K and the deposited amount was varied over three orders of magnitude from 0.3 to 300 ML. For erosion, a mass-selected ion beam of 1 keV Xe^+ was supplied by a differentially pumped ion source. The normal-incidence beam resulted in an erosion rate of 1 ML in 280 s. At the end of deposition or erosion, the sample was cooled to room temperature and imaged by scanning tunnelling microscopy (STM). STM images shown here are differentiated images. For large, greyscale topographs the height–height correlation function $G(\vec{r}) = \langle h'(\vec{x})h'(\vec{x}+\vec{r})\rangle$ with $h'(\vec{x}) = h(\vec{x}) - \bar{h}$ was determined, where $h(\vec{x})$ is the height of the surface at point $\vec{x}$ and $\bar{h}$ is the mean height. The surface roughness σ is given by $\sigma = \sqrt{G(0)}$. As the structure separation we used $\lambda = \frac{1}{2}(\lambda_1 + \lambda_2)$, where λ_1 is the double of the first zero of $G(\vec{r})$ [6], i.e. $\lambda_1 = 2|\vec{r}_1|$ with $G(\vec{r}_1) = 0$, while λ_2 is the quadruple of the full width at half-maximum of $G(\vec{r})$ [21], i.e. $\lambda_2 = 4|\vec{r}_2|$ with $G(\vec{r}_2) = \frac{1}{2}G(0)$.

In figure 1, same-size STM topographs after deposition of (*a*) 0.35 ML, (*b*) 3 ML, (*c*) 12 ML, and (*d*) 90 ML are presented, which show the evolution of the surface from two-dimensional islands to three-dimensional mounds. A number of qualitative features are obvious from the topographs: (i) the density of mounds and hence their average separation λ varies only slowly and remains almost constant from (*c*) to (*d*); (ii) from (*a*) to (*d*), the number of uncovered layers and thus also the surface roughness increases; (iii) as the average terrace width decreases from (*a*) to (*d*), no specific slope of mound walls is selected; (iv) in (*c*) and (*d*), deep grooves separating mounds are apparent; (v) in (*d*), there is an abrupt transition from mound slopes to flat mound tops; (vi) the larger the amount deposited, the less the steps at the mound tops deviate from the close-packed ⟨110⟩ orientation—indeed, for the top-layer islands, the kink density decreases from 20% in (*a*) to about 1% in (*d*).

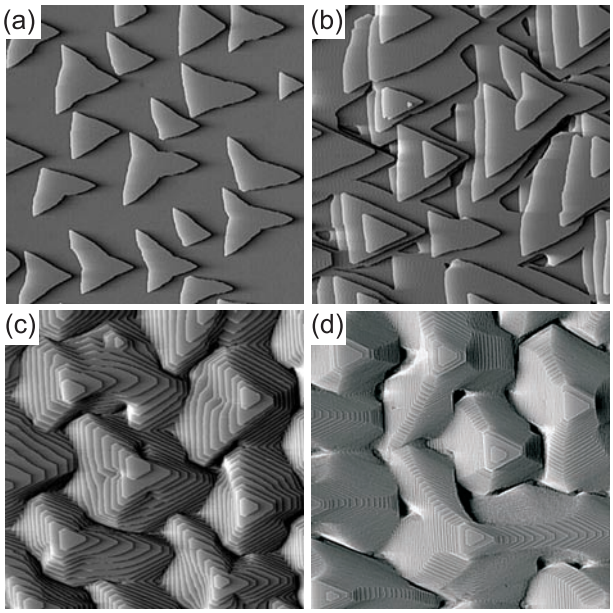

Figure 1. STM topographs of Pt/Pt(111) after growth at 440 K with $F = 7 \times 10^{-3}$ ML s^{-1}. (*a*) 0.3 ML, (*b*) 3 ML, (*c*) 12 ML, (*d*) 90 ML. The scan size in (*a*)–(*d*) is 2590×3450 Å^2.

The first three observations (i)–(iii) are substantiated by quantitative analysis. Figure 2(*a*) shows as open squares the surface roughness σ of the growth series partly represented in figure 1. For comparison, a dotted line is included which corresponds to a situation where the roughness develops as $\sigma = \Theta^{\beta}$ with $\beta = 0.5$. Initially, the roughness increases only slowly, then catches up, and for deposited amounts exceeding $\approx$10 ML the system indeed exhibits scaling behaviour with $\beta \approx 0.5$. In figure 2(*b*), the evolution of the mound separation λ is plotted as open squares. The separation increases initially, but saturates after a few ML have been deposited. A fit for the deposited amounts above 2.5 ML yields a growth exponent $1/z = 0.02 \pm 0.02$ ($\lambda \sim \Theta^{1/z}$). From these data, it is evident that the overall mound slope characterized by $\zeta = \sigma/\lambda$ increases continuously—no slope is selected up to 300 ML deposited.

If we disregard for the moment the data for deposited amounts <10 ML, excellent agreement with a one-dimensional model of an infinite step-edge barrier (Zeno model [22,23]) is obtained. In the model, the positions of the first-layer nucleation events essentially fix the positions of mounds evolving during subsequent deposition. Thermal adatom detachment from steps is forbidden and no coarsening is observed, i.e., $1/z = 0$. Due to the infinite step-edge barrier, the coverages of exposed layers obey a Poisson distribution and thus the roughness develops as $\sigma = \Theta^{0.5}$ (the dotted line in figure 2(*a*)) in fairly good agreement with the experiments. Finally, the model predicts an analytic form of the shape function which is in nearly perfect agreement with the experimental shape function [13]. Only the sharp needle mountain top of the analytic shape function differs markedly from the flat mountain tops observed in experiment (compare figure 1(*d*)). The reason for this difference is evident: each real system has only a finite step-edge barrier. Thus adatoms descend from the highest mound layer until the top terrace has reached a dimension such that the simultaneous presence of two adatoms becomes probable and eventually nucleation occurs.

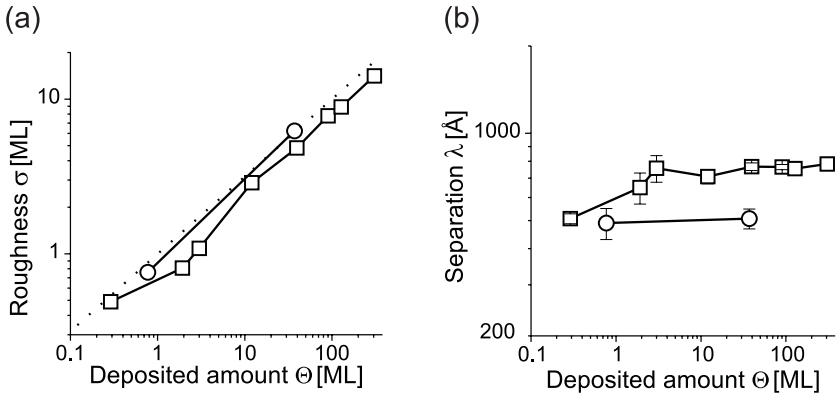

Figure 2. (*a*) Roughness σ and (*b*) mound separation λ versus the deposited amount Θ. Squares: growth at 440 K; circles: growth at 440 K with $P_{CO} = 2 \times 10^{-9}$ mbar. The lines are to guide the eye. Dotted line in (*a*): the analytical result for an infinitely high step-edge barrier. The error bars in (*a*) are below symbol size.

In view of the absence of coarsening for late-stage growth and for comparison with erosion discussed below, we note here that the compact island and mound shapes prove the presence of step-edge diffusion during growth. However, the absence of step fluctuations after deposition (verified directly by STM) shows that at 440 K the thermal creation of step adatoms from kinks is not possible on the experimental timescale. This excludes also step atom detachment.

What is the origin of the initial coarsening? Coalescence of two mounds by deposition noise may be expected after deposition of a number of particles onto an existing mound, which corresponds to the square of the number particles forming it [14]. Application of this concept to the initial growth on Pt(111) leads to coarsening amounts still orders of magnitude larger than actually observed. The importance of deposition noise for the initial coarsening can thus be ruled out. Funnelling, which has been observed in kinetic Monte Carlo (MC) simulations to induce coarsening [5, 7] is irrelevant as well, as due to the large island sizes at 440 K on Pt(111) the particle numbers funnelled are marginal. It is therefore postulated here that the initial coarsening is due to an initially low step-edge barrier, which gradually increases during growth, thereby inhibiting coarsening.

Indeed, the increase of the step-edge barrier height during growth can be quantified on the basis of our experiments. For islands it is possible to determine the hopping rate $\nu' = \nu'_0 e^{E_S/kT}$ over the edge barrier E_S by the analysis of the average island step-edge length L at which the probability of finding a second layer nucleus on top is $1/2$ by application of equation (34) of [24]. As for growth at 440 K, coalescence in the first layer takes place prior to nucleation in the second layer, only a lower bound for ν' is obtained at a coverage of about 0.8 ML. Using as the attempt frequency for going over the barrier the value $\nu'_0 = 7 \times 10^{11}$ Hz calculated [24] on the basis of the direct low-temperature field-ion-microscope measurements [25], one obtains $E_S \leqslant 0.33$ eV which translates into the additional step-edge barrier $\Delta E_S \leqslant 0.07$ eV (ΔE_S is the difference between E_S and the activation energy $E_D = 0.26$ eV for adatom hopping). A similar analysis for the sizes of terraces carrying the top-layer islands on mounds based on equation (46) of [24] yields the much larger value $\Delta E_S = 0.18 \pm 0.01$ eV after deposition of 90 and 301 ML. In a simple two-site model attributing a low value for the additional step-edge barrier to kink sites and a large value to sites in straight step edges, the drastic increase of the additional step-edge barrier is a consequence of the decrease in the kink concentration during growth [26], which is apparent in figure 1 and was noted under (vi) in the discussion above. This attribution

is consistent with previous calculations determining kink positions in the step edge to be the pathway for easy descent of adatoms from an island [27,28]. The reason for the decrease of the kink concentration with the deposited amount is as follows: due to the increasing step density during growth, fewer adatoms arrive at the edge per unit length and time. Thus step adatoms have more time to find existing kinks (and attach to them) instead of creating new kinks, e.g., by nucleation of step dimers. The way in which a low step-edge barrier leads to coarsening is the coalescence of adatom islands before a new adatom island is nucleated on top of each of them. This reduces the number of nucleation sites, as only one nucleus is formed on each coalesced terrace. In agreement with the preceding arguments, it is possible to suppress the initial coarsening for growth in the presence of a small CO partial pressure, which is known to cause a large step-edge barrier from the beginning of deposition [29] (compare the open circles in figure 2).

In order to reach a mound growth regime which exhibits mound coarsening, it would be desirable to increase the temperature of deposition significantly. However, for Pt(111) at temperatures of 500 K and above, the growth-induced reconstruction induces layer-by-layer growth [30], making mound coarsening studies impossible. Therefore, in the following, erosion experiments performed at temperatures of 600 K and above are described, which lead to pit formation. For the following it suffices to consider ion erosion as the inverse of homoepitaxial growth. Figures 3(*a*)–(*d*) exhibit STM topographs after removal of various amounts at 600 K. The morphology develops from monolayer-deep compact vacancy islands to regular hexagonal pits consisting of stacked vacancy islands and remainder pyramids and ridges in between. This evolution is driven by preferential nucleation of new vacancy islands at the bottom of existing ones. Figures 3(*e*)–(*h*) exhibit STM topographs (note the different scale) after removal of similar amounts, but at 750 K. In contrast to erosion at 600 K, at 750 K initially vacancy islands coalesce prior to nucleation of new vacancy islands on bottom terraces. Roughness builds up only slowly from remainders of coalesced layers (figures 3(*f*), (*g*)). As steps cannot pass by steps, these remainders pin steps also in subsequent removed layers (figure 3(*g*)) and eventually pits with large flat bottoms result (figure 3(*h*)). Although the roughness evolutions at the two temperatures are very different (in the STM topographs of figure 3 and also quantitatively as shown in figure 4), coarsening follows the same rule at 600 and 750 K. In fact for $\Theta > 10$ ML and the investigated temperatures of 600, 650, 700, and 750 K, a temperature-independent coarsening exponent $1/z = 0.28 \pm 0.02$ ($\lambda \sim \Theta^{1/z}$) is obtained.

The magnitude of this coarsening exponent is as expected from phenomenological theory for coarsening driven by surface diffusion currents. Step atom detachment which would create such a surface diffusion current cannot be responsible for the observed coarsening. Step atom detachment becomes relevant on the timescale of the experiment only between 650 and 700 K [18], while the coarsening is already observed for erosion at 600 K. Coarsening is proposed here to be due to efficient step-edge diffusion. Rapid step-edge diffusion could be inferred from shape transformations observed at 600 K [18] and the always hexagonal pit shape. The edge diffusion mechanism for pit coarsening (similar to the one proposed for mound coarsening [14]) is sketched in the cartoons of figure 5. After coalescence (figure 5(*a*)), the line tension of the new common step of the joint island causes the step to approach again a compact shape, enabled by step-edge diffusion. Thereby it starts to interact with the two vacancy islands in the bottom terrace, moving them towards their common centre of mass (see figure 5(*b*)). Step-edge-diffusion-induced position and shape fluctuations of the bottom-layer islands [31] allow them to approach in reaction to the position of the upper-layer island. The upper-layer step may exert forces on the vacancy island by step–step repulsion, known to be strong on Pt(111) [32]. In the absence of step–step repulsion upper- and lower-layer steps may even touch, resulting in material transport from the upper to the lower layer. These processes eventually lead to coalescence of the bottom-layer vacancy islands prior to nucleation of new

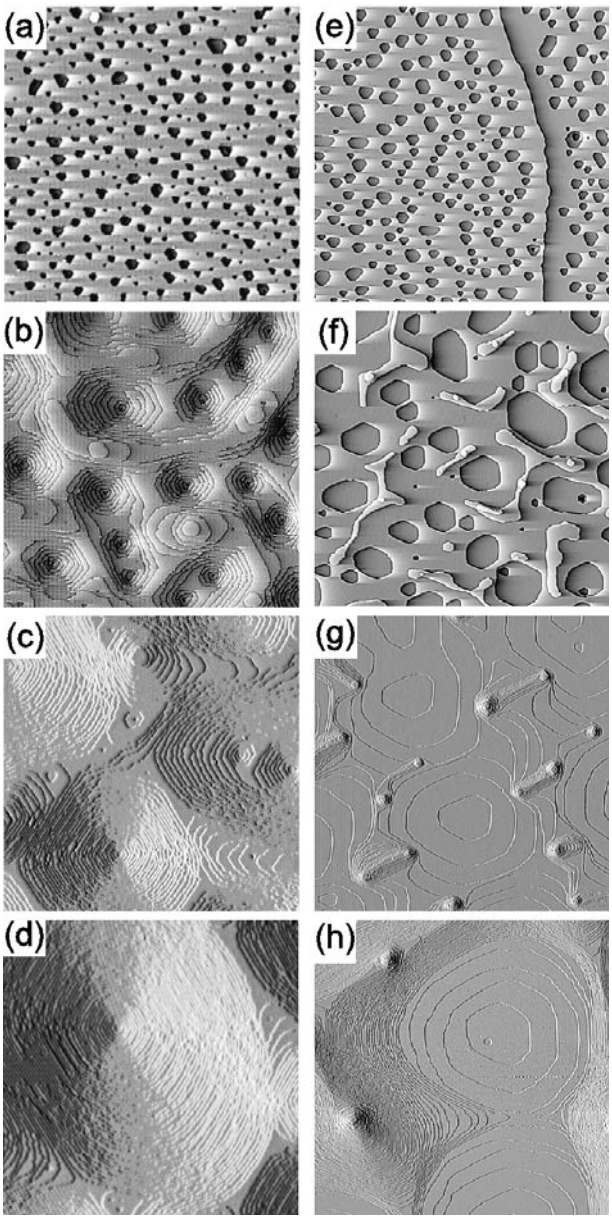

Figure 3. STM topographs after erosion of (*a*) 0.26 ML, (*b*) 6.2 ML, (*c*) 66 ML, and (*d*) 333 ML at 600 K and of (*e*) 0.24 ML, (*f*) 6.3 ML, (*g*) 65 ML, and (*h*) 601 ML at 750 K. Topograph width: 810 Å for (*a*)–(*d*) and 3460 Å for (*e*)–(*h*).

islands at both of their bottoms. If after coalescence only one island is left on the bottom terrace, the process is finished. Rapid rearrangement by edge diffusion in all layers will lead to a single pit consisting of stacked hexagonal vacancy islands. Figure 5(*c*) shows a typical situation, for which the above-described scenario applies.

We performed kinetic 3D lattice MC simulations [20] for ion erosion of a fcc (111) surface. The simulations are performed at 500 K in a linear nearest-neighbour model, which reproduces

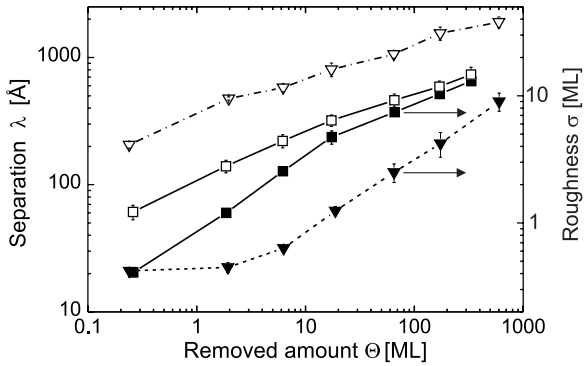

Figure 4. The dependences of the feature separation λ (left y-axis) and roughness σ (right y-axis) on the removed amount Θ at 750 K (downward-pointing triangles and dashed curves) and 600 K (squares and full curves). Full symbols for σ and open symbols for λ. The curves are to guide the eye.

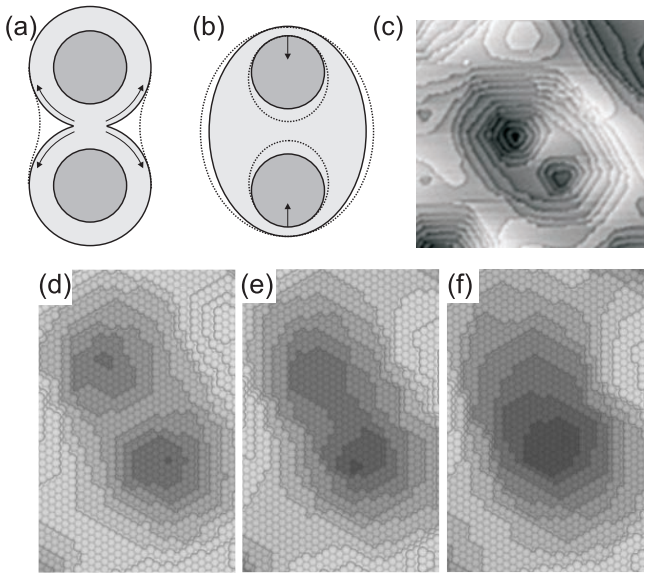

Figure 5. (*a*), (*b*) Schematic sketches of the mechanism of coarsening by step-edge diffusion (see the text). (*a*) Immediately after the coalescence of two vacancy islands a strong edge diffusion current moves material away from the locations of high curvature. (*b*) During shape rearrangement in response to the step line tension, the coalesced islands approach the two bottom vacancy islands, starting to move them towards their common centre of mass. (*c*) A STM topograph of two sub-pits in the process of coalescence. Topograph size: 500 Å; 6.2 ML removed at 600 K. (*d*)–(*f*) Snapshots of the MC simulation showing a pit coalescence event. The removed amounts are (*d*) 3.2 ML, (*e*) 3.85 ML, and (*f*) 4.2 ML.

the hierarchy of diffusion processes on Pt(111) adequately. The activation barrier for a process results from the difference in coordination (bond strength 0.25 eV) of initial and final states, and an additional fixed kinetic barrier for all processes (0.5 eV). The bond strength and kinetic barrier are adjusted to reproduce the correct experimental erosion and annealing behaviour at about 600 K. It is checked that step atom detachment is insignificant under these conditions.

In order to explicitly test for the relevance of step-edge diffusion, additional simulations with two different *ad hoc* rules were performed. First, explicit suppression of atom detachment from steps in the simulation does not change coarsening behaviour compared to the standard simulation and results in $1/z = 0.22$. Second, kinks were made irreversible traps for atoms. This allows step adatoms resulting from the bombardment to still migrate along densely packed steps until they are trapped in a kink position, but thermal creation of step adatoms from kinks is suppressed. This *ad hoc* rule diminished coarsening substantially and an exponent of $1/z = 0.09$ resulted. The MC simulation thus indicates as key process for coarsening the thermal formation of step adatoms from kinks. In figures 5(*d*)–(*f*) three snapshots of a typical pit coarsening process are shown. Figure 5(*d*) shows two sub-pits surrounded by three common steps. Periodically, the narrow separation between the sub-pit top-layer vacancy islands breaks and the islands rearrange. Immediately before the snapshot of figure 5(*e*) the last of these break events took place, finishing the pit coalescence. The two coalesced islands are seen in figure 5(*e*) just in the processes of reshaping. As is apparent from figure 5(*f*), subsequently all the steps forming the pit approach a more compact, hexagonal shape [33].

At first glance the observations for growth of Pt on Pt(111) at 440 K appear to contradict the coarsening mechanism proposed here for erosion of Pt(111): although the regular mound shapes in growth demonstrate the existence of step-edge diffusion, coarsening is largely absent. In fact, at 440 K adatoms reaching the step edge and becoming step adatoms may efficiently migrate along densely packed steps and around corners until they are irreversibly incorporated at kink sites. While this step-edge diffusion leads to regular island and mound shapes, in the absence of the deposition flux the morphology freezes entirely. Only at about 500 K does step-edge diffusion in the absence of a particle flux become relevant on the timescale of the experiment: mobile step adatoms are created thermally by emission from kinks [34,35]. Only these mobile species allow the system to react rapidly to differences in chemical potential along step edges and thus lead to coarsening. We find thermal step adatom creation by emission from kinks to be the key process for coarsening, in full agreement with the MC simulations.

Bond counting for fcc (111) and hcp (0001) surfaces tells us that the thermal mobility along step edges (including the formation of step adatoms and their transport around corners) involves one bond less broken than the thermal formation of adatoms. Therefore one may speculate that the observed coarsening in homoepitaxy on Rh(111) [36] at 725 K and erosion of Au(111) [11] above 295 K are due to step-edge diffusion including creation of mobile species rather than step atom detachment. Considering nearest- and next-nearest-neighbou bonding, similar reasoning may be applied to surfaces with square symmetry (e.g. fcc (001)).

The present experiment highlights two difficulties in the application of phenomenological models to surface evolution under growth or erosion. First, the diffusion current driven by differences in chemical potential of the surface atoms is not just proportional to the gradient of surface curvature; i.e. the expression $\vec{j}_{eq} \sim \vec{\nabla}(\nabla^2 h)$ is not valid in general. If e.g. only step-edge diffusion is active, it is evident that it is not the gradient of the curvature but only the component of the gradient along the height contour that determines the surface diffusion current. For a description of surface diffusion it may therefore be more appropriate to split the surface current locally into components normal and parallel to the height contours as $\vec{j} = (j_{\perp detach}; j_{\parallel detach} + j_{\parallel edge})$, which are then determined by changes in curvature normal and parallel to the contour lines. Due to the kinetic coefficients involved, the two components may depend differently on the magnitude of the curvature change. Second, as nucleation is not included in phenomenological theory, it is not able to predict the presence of flat surface areas, which always appear when nucleation is difficult. The size of these flat areas in growth is directly linked to the step-edge barrier

for adatoms [24], while in ion erosion the situation is more difficult: here their size is linked to the efficiency of step atom detachment, effectively short-circuiting the step-edge barrier for vacancies [18, 19].

In conclusion, coarsening of pits in erosion of Pt(111) is due to step-edge diffusion including thermal creation of step adatoms from kink positions. This mechanism is likely to be operative, in erosion as well as growth, also on other low-index metal surfaces. Step-edge diffusion during growth without thermal creation of mobile species does not generally allow coarsening. Only for low step-edge barriers, even under these conditions, is initial coarsening by coalescence of islands possible.

Acknowledgments

We thank Joachim Krug for useful discussions and Carsten Busse for critically reading the manuscript. TM acknowledges support by the Deutsche Forschungsgemeinschaft.

References

[1] Cherns D 1997 *Phil. Mag.* **36** 1429
[2] Villain J 1991 *J. Physique* I **1** 19
[3] Krug J, Plischke M and Siegert M 1993 *Phys. Rev. Lett.* **70** 3271
[4] Siegert M and Plischke M 1994 *Phys. Rev. Lett.* **73** 1517
[5] Šmilauer P and Vvedensky D D 1995 *Phys. Rev.* B **52** 14 263
[6] Stroscio J A, Pierce D T, Stiles M D and Zangwill A 1995 *Phys. Rev. Lett.* **75** 4246
[7] Amar J and Family F 1996 *Phys. Rev.* B **54** 14 742
[8] Zuo J K and Wendelken J F 1997 *Phys. Rev. Lett.* **78** 2791
[9] Poelsema B, Kunkel R, Verheij L K and Comsa G 1990 *Phys. Rev.* B **41** 11 609
[10] Costantini G, Rusponi S, Gianotti R, Boragno C and Valbusa U 1998 *Surf. Sci.* **416** 245
[11] Murty M V R, Curcic T, Judy A, Cooper B H, Woll A R, Brock J D, Kycia S and Headrick R L 1998 *Phys. Rev. Lett.* **80** 4713
[12] Siegert M 1998 *Phys. Rev. Lett.* **81** 5481
[13] Kalff M, Comsa G and Michely Th 1999 *Surf. Sci. Lett.* **426** L447
[14] Tang L H, Šmilauer P and Vvedensky D D 1998 *Eur. Phys. J.* B **2** 409
[15] Schinzer S, Kinne M, Biehl M and Kinzel W 1999 *Surf. Sci.* **439** 191
[16] Amar J 1999 *Phys. Rev.* B **60** R11 317
[17] Moldovan D and Golubovic L 2000 *Phys. Rev.* E **61** 6190
[18] Michely Th, Kalff M, Comsa G, Strobel M and Heinig K H 2001 *Phys. Rev. Lett.* **86** 2592
[19] Kalff M, Michely Th and Comsa G 2001 *Surf. Sci.* **486** 103
[20] Strobel M, Heinig K H and Michely Th 2001 *Surf. Sci.* **486** 136
[21] Rost M, Šmilauer P and Krug J 1996 *Surf. Sci.* **369** 393
[22] Elkinani I and Villain J 1993 *Solid State Commun.* **87** 105
[23] Krug J 1997 *J. Stat. Phys.* **87** 505
[24] Krug J, Politi P and Michely Th 2000 *Phys. Rev.* B **61** 14 037
[25] Kyuno K and Ehrlich G 1998 *Phys. Rev. Lett.* **81** 5592
[26] Michely Th, Kalff M and Comsa G 2002 in preparation
[27] Villarba M and Jónsson H 1994 *Surf. Sci.* **317** 15
[28] Jacobsen J, Jacobsen K W and Nørskov J 1995 *Phys. Rev. Lett.* **74** 2295
[29] Kalff M, Comsa G and Michely Th 1998 *Phys. Rev. Lett.* **81** 1255
[30] Michely Th, Hohage M, Esch S and Comsa G 1996 *Surf. Sci. Lett.* **349** L89
[31] Rosenfeld G, Morgenstern K, Esser M and Comsa G 1999 *Appl. Phys.* A **69** 489
[32] Hahn E, Schief H J, Marsico V, Fricke A and Kern K 1994 *Phys. Rev. Lett.* **72** 3378
[33] http://www.fz-rossendorf.de/FWI/FWIT/ion_eros.htm
[34] Feibelman P J 1999 *Phys. Rev.* B **60** 4972
[35] Giesen M, Schulze Icking-Konert G, Stapel D and Ibach H 1996 *Surf. Sci.* **366** 229
[36] Tsui F, Wellman J, Uher C and Clarke R 1996 *Phys. Rev. Lett.* **76** 3164